Electronic Supplementary Information

Self-assembly of robust graphene oxide membranes with chirality for highly stable and selective molecular separation

Yufan Zhang,[a,b§] Zehai Xu,[a§] Tingting Zhang,[a§] Qin Meng,[c] Xu Zhang,[a] Chong Shen,[c] Yinghua Lu,[c] Guoliang Zhang*[a] and Congjie Gao [a]

[a] *Institute of Oceanic and Environmental Chemical Engineering, Center for Membrane and Water Science &Technology, State Key Lab Base of Green Chemical Synthesis Technology, Zhejiang University of Technology, Hangzhou 310014, China.*

[b] *College of Engineering, Carnegie Mellon University, Pittsburgh, PA 15213, USA.*

[c] *College of Chemical and Biological Engineering, State Key Laboratory of Chemical Engineering, Zhejiang University, Hangzhou 310027, P. R. Ch*ina.

[d] *College of Chemistry and Chemical Engineering, National Laboratory for Green Chemical Productions of Alcohols, Ethers and Esters, Xiamen University, Xiamen, 361005, P. R. China.*

*Corresponding author E-mail: guoliangz@zjut.edu.cn

Experimental

Chemicals and materials

The natural graphite flakes (500 mesh), methyl Orange (MO), methylene blue (MB), basic red 18 (BR18), reactive red X-3B were purchased from market. $KMnO_4$, NaOH and $NaNO_3$, levodopa, d-3,4-dihydroxyphenylalanine (DDA), hydrogen peroxide (H_2O_2, 30 wt.%), L-leucine and tri-hydroxymethyl aminomethane (Tris) were all of analytical grade. All the regents were used as received. All experiment solutions were prepared from deionized water manufactured by a RO-EDI system.

Corresponding formula

The formula of pure water flux and rejection of dyes are depicted as follows:

$$\mathrm{F} = \frac{Q}{A \times \mathrm{t}}$$

$$\mathrm{R}(\%) = (1 - \frac{C_1}{C_2}) \times 100$$

where F represents the pure water flux (m^3 m^{-2} s^{-1}), Q represents the quantity of permeate (m^3), t represents the permeation time (s) and A represents the effective membrane area (m^2), R represents the dye rejection ratio (%), C_1 represents the concentration of dye in permeate (g/L), C_2 represents the concentration of dye in feed (g/L).

Table S1. The compositions of hybrid solutions and mechanical parameters of different membranes.

Membrane type	GO (g/L)	LDA (g/L)	Young' s modulus (Gpa)	Hardness (Gpa)
N0	0.1	\	3.23±1.32	0.3±0.05
N1	0.1	0.1	15.58±1.67	0.46±0.05
N2	0.1	0.2	22.62±2.04	0.71±0.08
N3	0.1	0.4	14.97±1.58	0.40±0.02
N4	0.1	0.8	6.23±1.22	0.37±0.03

The nanoindentation was employed to assess the mechanical properties of prepared membranes. As depicted in Table S1, N2 membrane exhibits the highest Young's modulus (22.62±2.04 Gpa) and hardness (0.71±0.08 Gpa), the value of Young's modulus is 7 times higher than that of N0 membrane. However, a sharp decrease in mechanical properties occurred with higher LDA loading, which can be attributed to the aggregation of PLDA and the increase of rGO-PLDA interfacial area, similar to previous report.[28, S1]

Table S2. Comparison of permselectivity of different GO-based membranes.

GO-based membrane	Test method	Permeance ($m^3\ m^{-2}\ s^{-1}\ bar^{-1}$)	Rejection (%)	Thickness (nm)	Operation time (h)	Ref
BPEI/GO	dead-end	6.63×10^{-7}	96.4	60	\	32
GO/graphene	dead-end	1.67×10^{-6}	97.6	214	\	44
GO-mPDA	dead-end	1.63×10^{-6}	\	600	6	45
GO@PAN	dead-end	2.77×10^{-7}	99.9	600	0.75	46
TiO_2@GO	dead-end	1.00×10^{-6}	98.0	39.7	9	47
N1	cross-flow	1.80×10^{-6}	99.9	350	170	This work

Table S3. Comparison of the performance of different membranes in different conditions.

Graphene-based membrane	Test method	Mark molecules	molecular weight	Concentration (mg L^{-1})	Rejection/%	Pressure (bar)	Ref
BPEI/GO	dead-end	MB	319 (+)	10	96.4	5	32
PNIPAM/CCG (3:1)/NME	dead-end	RhB	479 (+)	\	70	1	30
GO–TMC/PSF	dead-end	MB	373 (+)	7.5	66	3.4	S2
		R-WT	487 (-)	7.5	95		
GO/FLG	cross-flow	RhB	479 (+)	\	8	6	28
		Acid Blue 9	792 (-)	\	96		
N1	cross-flow	MO	327 (-)	100	93.3	1	This work
		MB	373 (+)	100	99.9		
		BR18	390 (+)	100	99.7		
		X-3B	615 (-)	100	99.1		

Compared with the reported graphene-based nanofiltration for dye rejection, the prepared rGO/PLDA composite membranes exhibited prominent rejection for both positively and negatively small molecules, even in very high dye concentration of 100 mg/L.

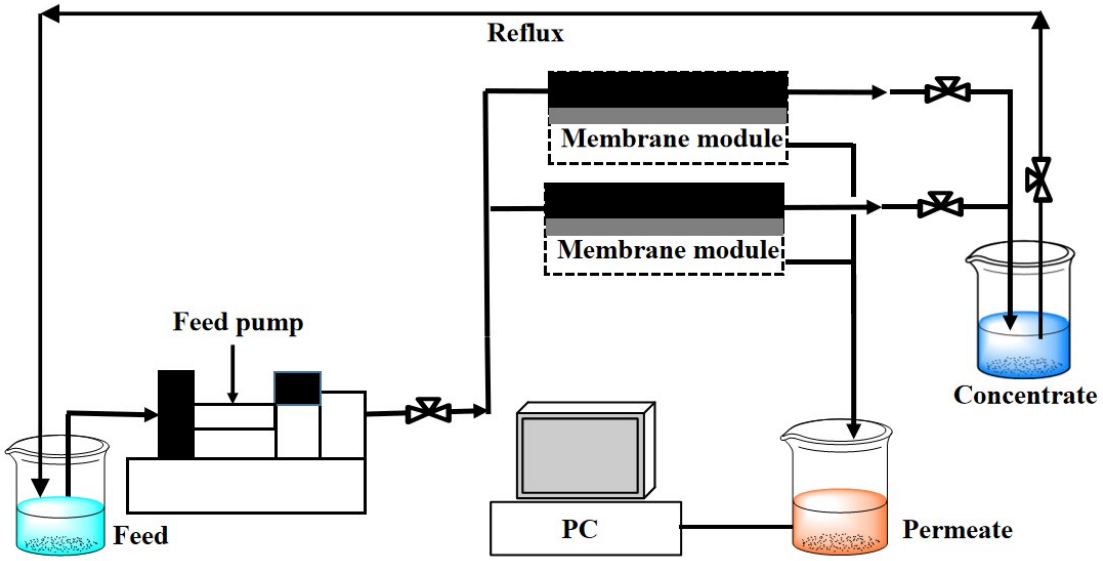

Figure S1. Schematic of cross-flow nanofiltration process.

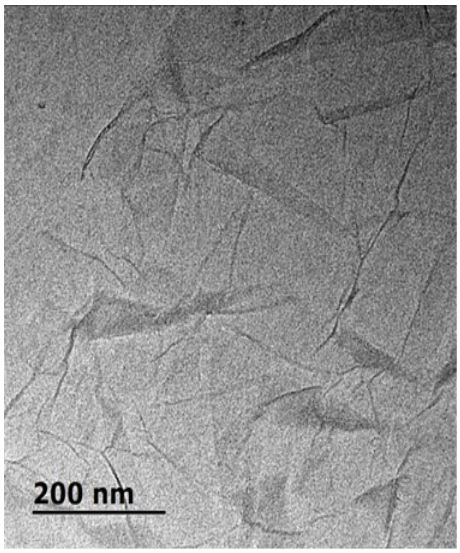

Figure S2. TEM image of prepared rGO nanosheets**.**

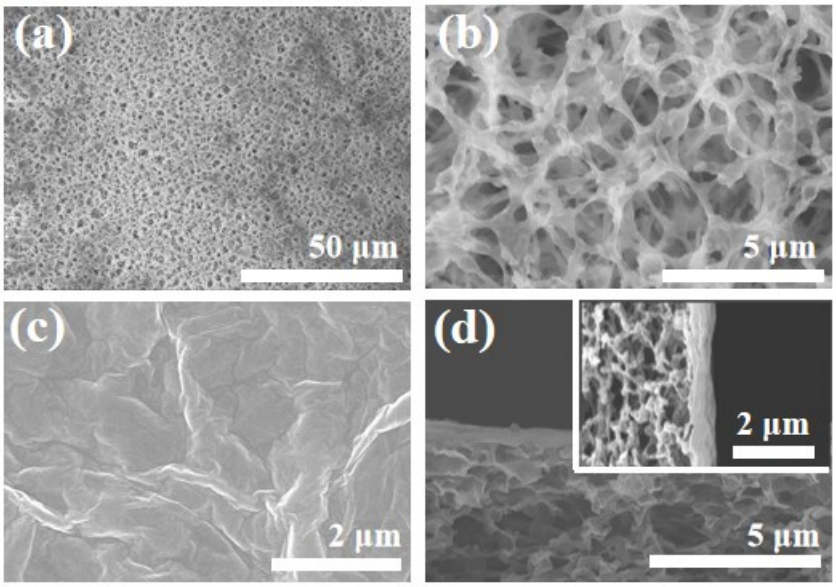

Figure S3. SEM images of the surface of the CA substrate (a,b) and N0 membrane (c,d). From the image, uniform microporous structure of cellulose ester commercialized microporous filtration substrate is shown. After coating GO layer, typical wrinkles on the surface can be observed obviously.

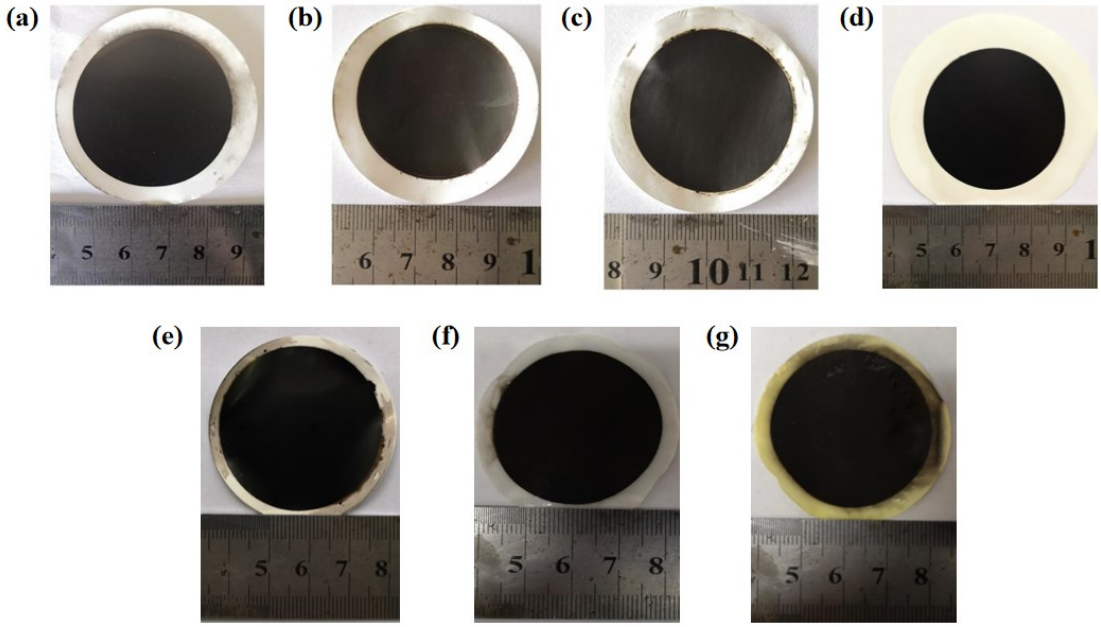

Figure S4. Photographs of prepared rGO/PLDA composite membranes. Different kinds of rGO/PLDA composite membranes were synthesized by using CA (a), Nylon (b), PVDF (c), PES (d), PE (e), PAN (f) and hydrolyzed PAN (g) microfiltration membranes as substrates. As shown in the figure, the chiral PLDA with catechol and indole functional groups has a strong adhesion with support,[S3] resulting in the rGO/PLDA layer's firm location on different polymer substrates.

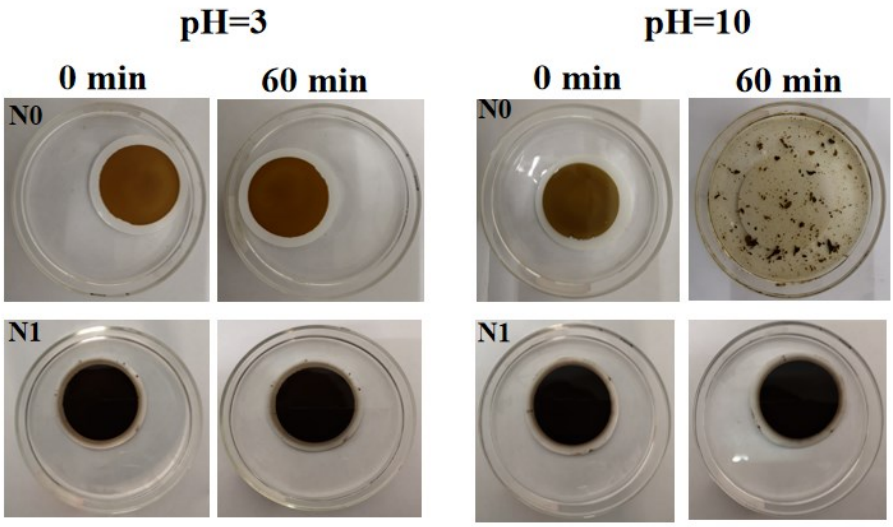

Figure S5. Digital photos of N0 and N1 membranes soaked in aqueous solution at pH=3 and pH=10, respectively.

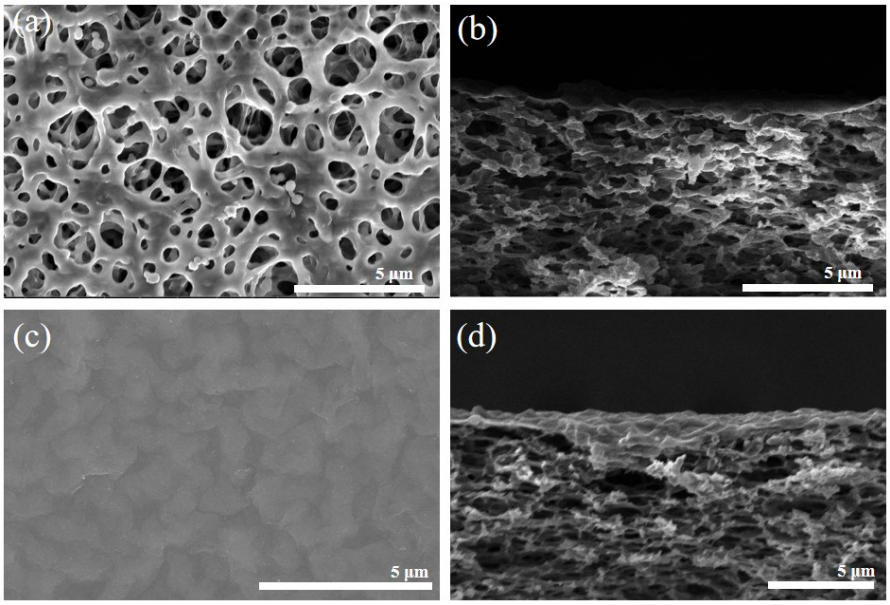

Figure S6. Surface and cross-section SEM images of N0 membrane (a, b) and N1 membrane (c, d) after soaking in water at pH=10.

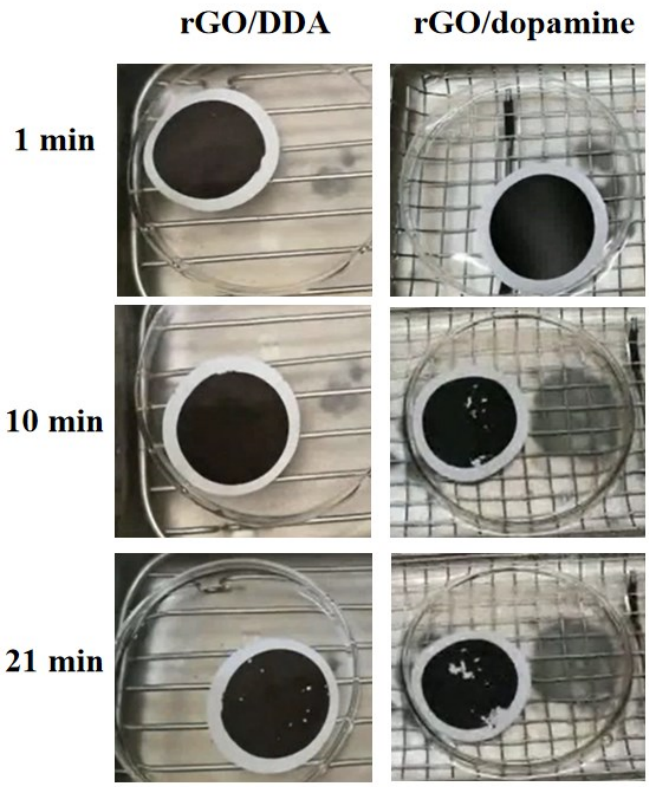

Figure S7. Photo graphs of rGO/DDA and rGO/dopamine membranes under sonication treatment with different time.

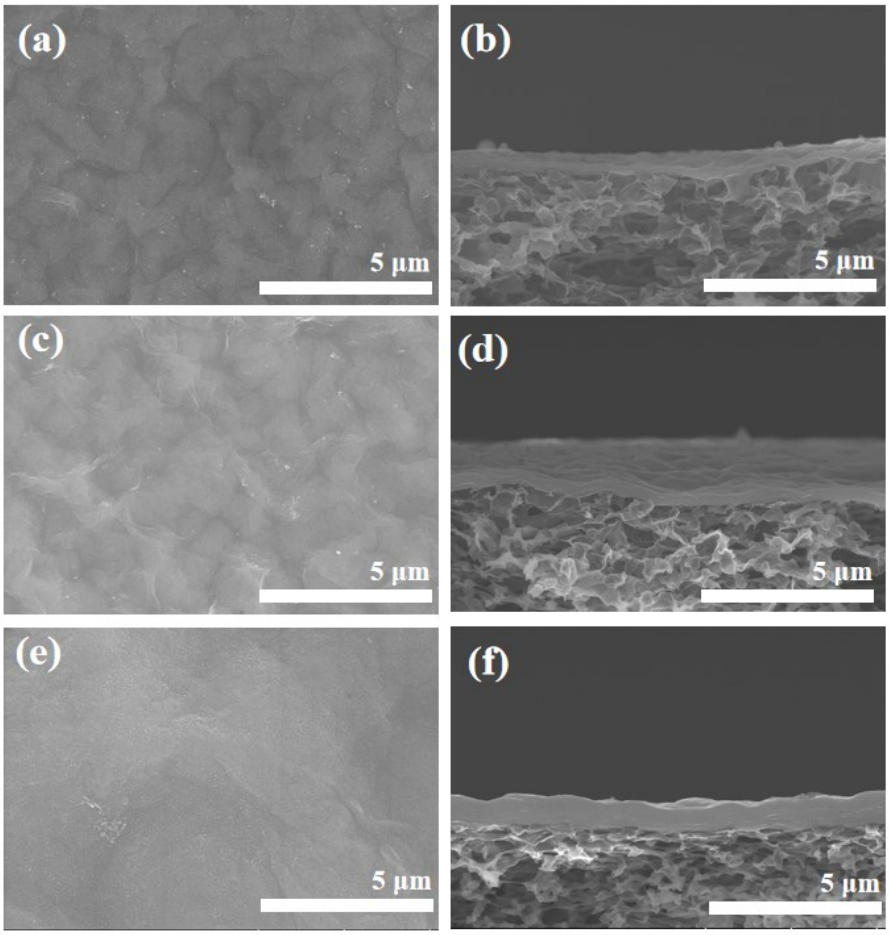

Figure S8. Surface and cross-section SEM images of different rGO/PLDA membranes after cross-flow filtration for a cycle of 8 hours. (a, b) N2 membrane; (c, d) N3 membrane; (e, f) N4 membrane.

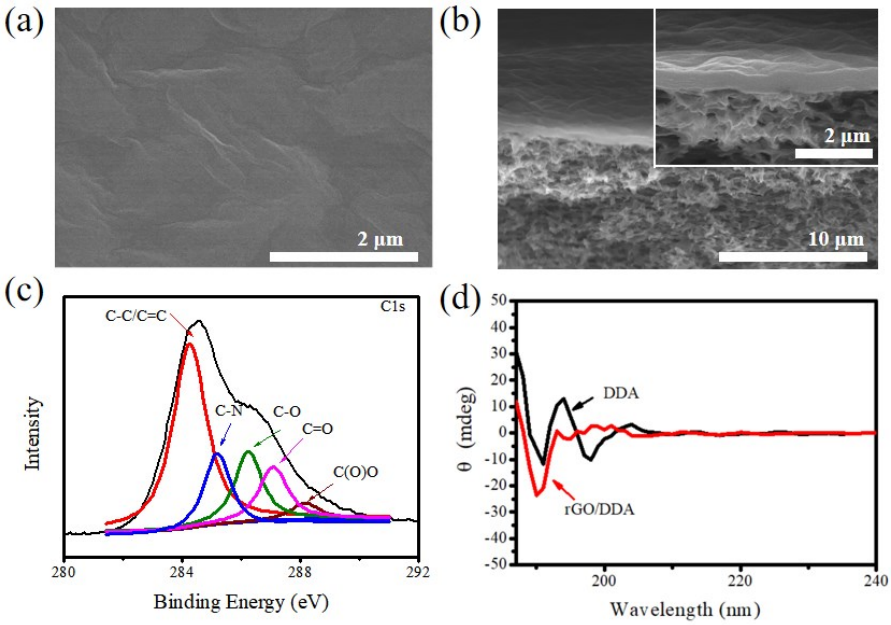

Figure S9. (a, b) Surface and cross-section of SEM images of rGO/DDA membrane. (c) CD spectra of DDA and rGO/DDA. (d) C 1s spectra of the synthesized rGO/DDA composite membrane. From the CD spectra, the intensity of peaks of rGO/DDA samples was higher than that of DDA, revealing chiral amplification compared with rGO/PLDA sample.

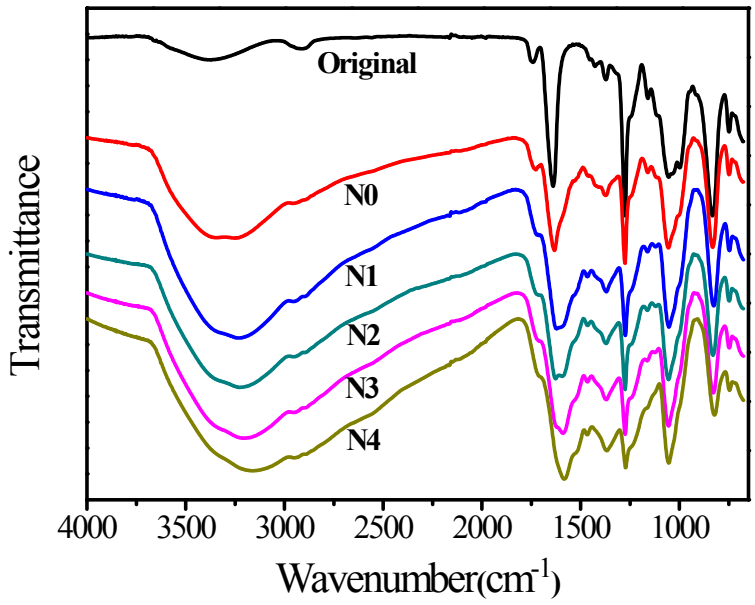

Figure S10. FTIR spectra of different prepared membranes. There was a major dependence of the property of composite membranes on the strong cross-linking interaction between chiral PLDA and rGO nanosheets. In the chiral PLDA cross linked rGO nanosheets, there existed three types of bonds between chiral PLDA and rGO: hydrogen-bonding interaction between amino in PLDA molecules and oxygen containing functional groups in rGO, ionic bonding in protonating amine and carboxyl and the most strong covalent bonding among amine and oxygen containing groups by nucleophilic substitution reactions.[S4] Although hydrogen bond and ionic bond was a little bit weaker, the formed covalent bonds could still maintain their structural integrity under aggressive cross-flow in nanofiltration processes.

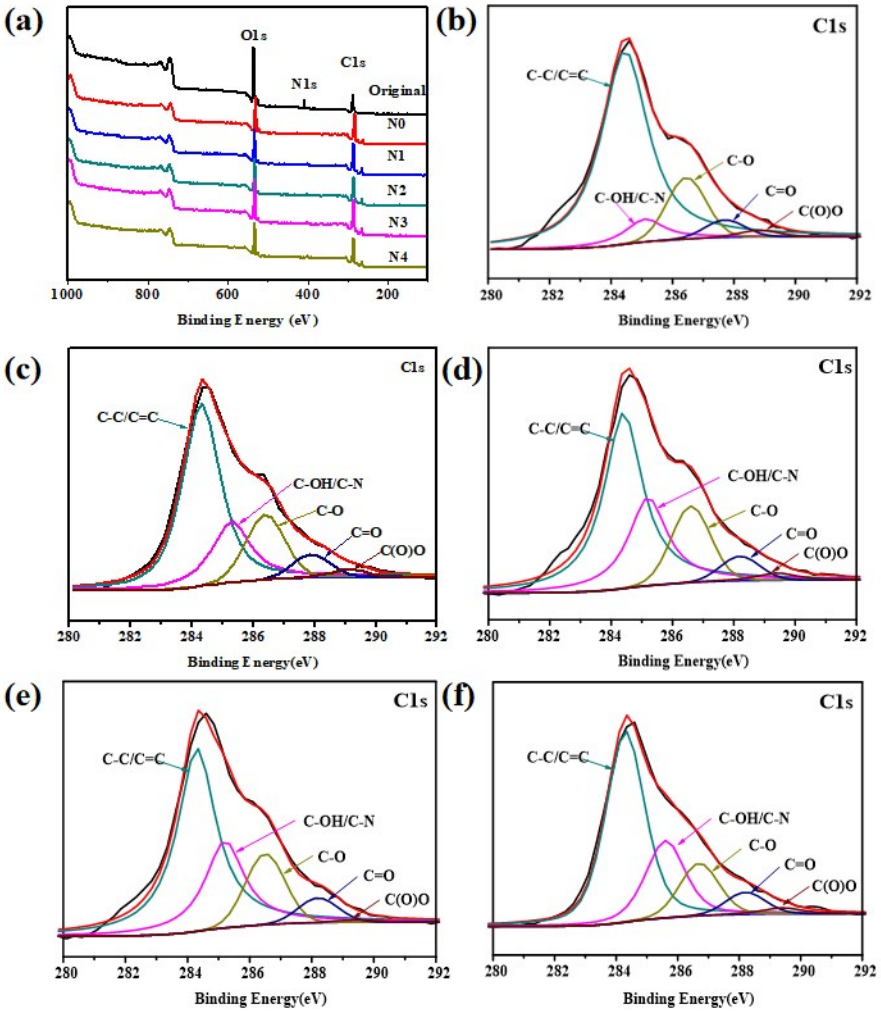

Figure S11. XPS survey spectra. full spectra (a). C 1s spectra of the synthesized membranes: N0 membrane (b), N1 membrane (c), N2 membrane (d), N3 membrane (e) and N4 membrane (f). In the binding region of C 1s spectrum, a part of functional groups on GO nanosheets might be consumed in the reactions with amine molecules, which should be associated with the nucleophilic substitution reaction. The amine groups were then motivated to attack the oxygen containing functional groups to form covalent bonds between C-O/O-C=O and C-N-R,[S5] which is consistent with the results obtained from the FTIR spectra.

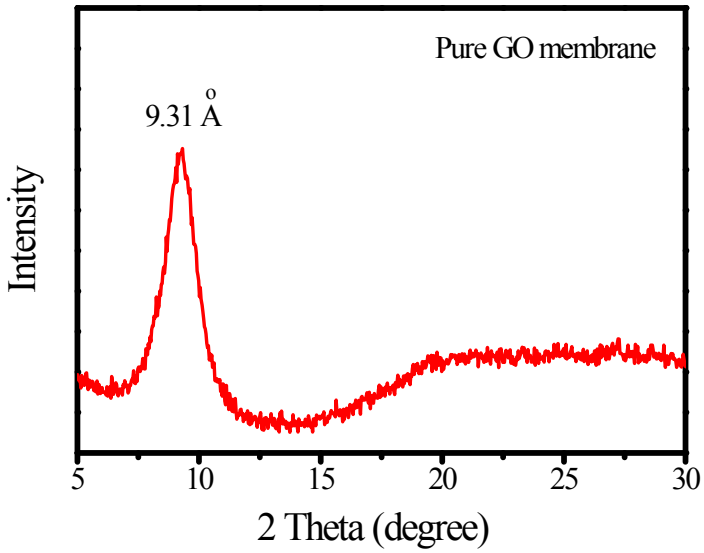

Figure S12. XRD pattern of pure GO membane in dry condition.

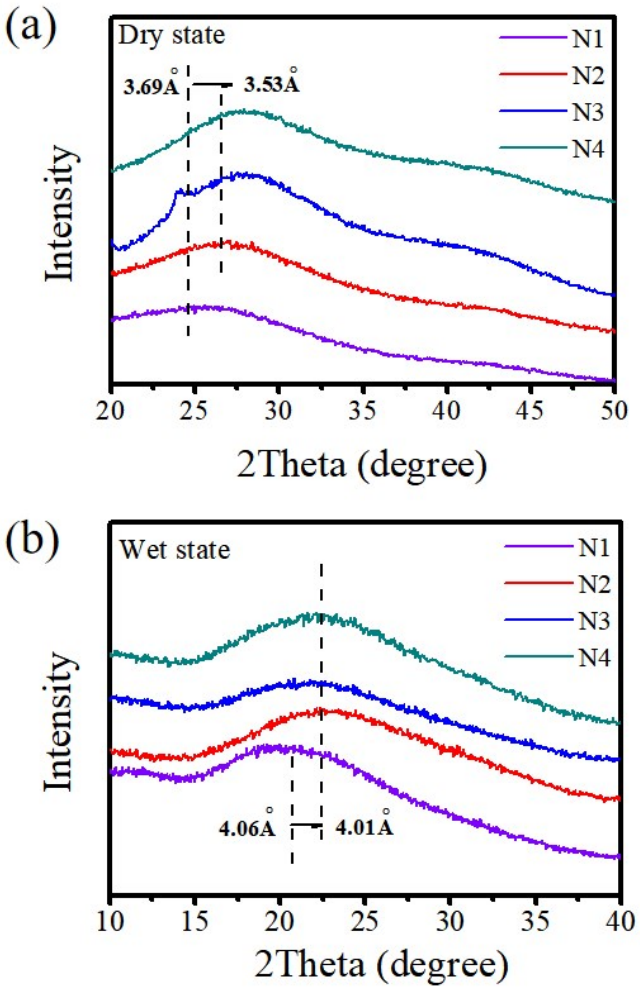

Figure S13. XRD patterns of rGO/PLDA membranes in dry state (a) and wet state (b).

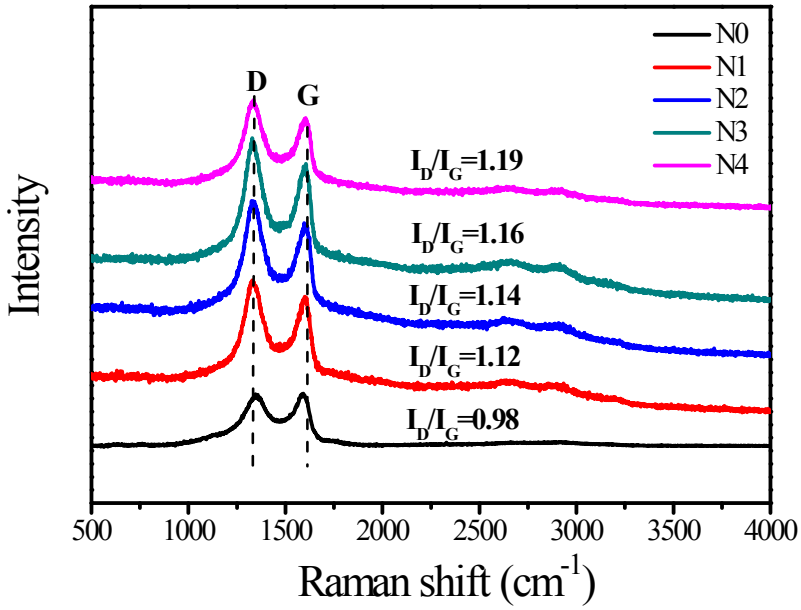

Figure S14. Raman spectra of pure GO and rGO/PLDA membranes.

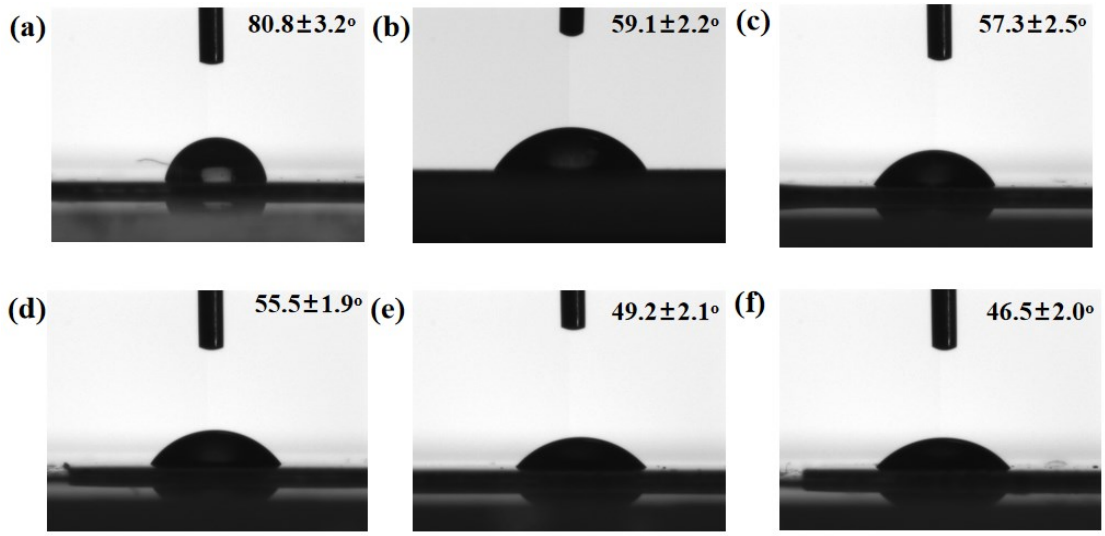

Figure S15. Contact angle measurements of water on the surfaces of different membranes. (a) CA support, (b) N0 membrane, (c) N1 membrane, (d) N2 membrane, (e) N3 membrane, (f) N4 membrane. The result demonstrated that the hydrophilicity of rGO/PLDA membranes was gradually enhanced after increasing the content of chiral LDA. After deposition of chiral rGO/PLDA composites, the prepared nanofiltration membranes showed much smaller contact angles compared to CA substrate.

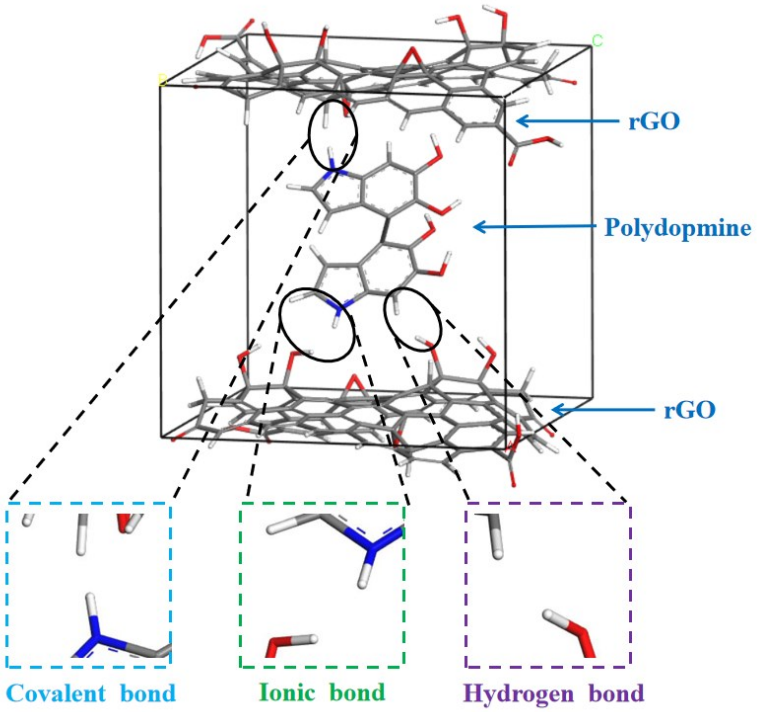

Figure S16. Three dimensional view of an amorphous cell of polydopamine molecule between two rGO nanosheets after equilibrium calculation**.**

References:

S1 L. Cseri, J. Baugh, A. Alabi, A. AlHajaj, L. Zou, R. A. W. Dryfe, P. M. Budd, G. Szekely, *J. Mater. Chem. A* 2018, **6**, 24728.

S2 M. Hu, B. Mi, *Environ. Sci. Technol.* 2013, **47**, 3715.

S3 Z. H. Xu, S. J. Ye, G. Zhang, W. B. Li, C. J. Gao, C. Shen, Q. Meng, *J. Membr. Sci*. 2016, **509**, 83.

S4 R. C.-S. Laura, J. Cote, J. Huang, *J. Am. Chem. Soc.* 2009, **131**, 11027.

S5 S. Xia, M. Ni, T. Zhu, Y. Zhao, N. Li, *Desalination* 2015, **371**, 78.